Attenuation of Vibration and Mass Reduction using a Finite Hollow Periodic Rod

Jean P. Carneiro Jr.[1], Vinicius G. Cleante[1], Paulo J. P. Gonçalves[2], Michael J. Brennan[1]

[1] *School of Engineering, State University of São Paulo*
Av. Brasil Sul, 56, 15385-000, Ilha Solteira/São Paulo, Brazil
jean.carneiro@unesp.br, vinicius.cleante@unesp.br, mjbrennan0@btinternet.com
[2] *School of Engineering, State University of São Paulo*
Av. Eng. Luís Edmundo Carrijo Coube, 14-01, 17033-360, Bauru/São Paulo, Brazil
paulo.paupitz@unesp.br

Abstract. Through the decades, periodic structures have been studied using different models and configurations, and recently, metamaterial design has emerged as a hot topic for research. The effect of creating pass and stop bands for this type of system considerably expands the possibility of applications. However, there is a knowledge gap regarding practical analysis, which relates attenuation gains with physical properties, such as structural mass. This work presents a design improvement to increase vibration attenuation and mass reduction for a periodic rod. Asymmetric cells are considered using solid and hollow configurations. Using the transfer matrix method, displacement transmissibility expressions are derived as a function of the internal diameter. Numerical simulations show that a structure with hollow cells results in a reduction of 24% in the minimum transmissibility and a reduction in mass of about 40%, compared to a similar structure with solid cells.

Keywords: Periodic structures, transfer matrix approach, asymmetric structures.

1 Introduction

In vibration control problems, the transmission element between source and receiver is frequently modified. This can involve a periodic structure, which can be tuned so that there are frequency ranges in which wave propagation is significantly attenuated [1,2].

In the literature, there are numerous applications of periodic structures. A phonic crystal was applied to vehicle bodies to reduce the total vibration [3,4]. Vibration tests have demonstrated the potential use of periodic structures to satellite panels so that they can endure vibration loads during the rocket launch [5]. Numerical and experimental results based on both the spectral finite element method and the transfer matrix method showed improvement in the acoustic comfort of helicopter cabins employing periodic structures [6,7].

In any structure designed to attenuate vibration, there are design requirements and physical limitations. However, most studies involving periodic structures, focus on the characterisation of infinite structures, which can obscure additional effects. It has been demonstrated that finite periodic structures have wider attenuation bands greater than the stop band of an infinite structure, but for a large number of cells these two frequency bands converge [8,9]. There is scant literature regarding practical analysis in this context, but some work has considered the problem of minimising the total mass, but without considering the arrangement of a periodic structure [10].

This aim of this paper is to investigate whether the geometry of a periodic structure can be arranged, such that mass can be removed from a structure, but the vibration isolation performance is improved. To this end a rod-like periodic structure is considered and the transfer matrix approach employed to determine the vibration transmission through the structure, as described in [11,12].

2 Problem statement

A finite array of periodic rods is constructed from the successive repetition of N cells, as shown in Fig. 1. The vibration transmission though the structure can be quantified by the ratio of the displacement ratio at the right-end side of the last cell $U_R^{[N]}$ to the displacement at the left-end side of the first cell $U_L^{[1]}$. This is called the displacement transmissibility. In the study of a finite periodic array of rods, it has been demonstrated that it is advantageous to use asymmetric rather than symmetric cells [12]. Moreover, it has been shown that it is important to orientate the cells so that the thinner rod section within a cell is closer to the source (the left-hand end in this case).

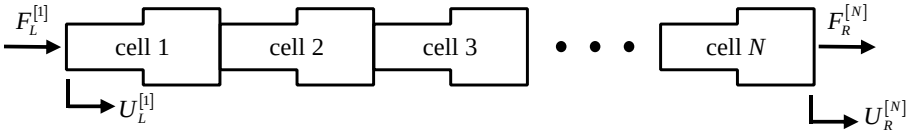

Figure 1. Finite structure consisting of N asymmetric periodic cells.

Figure 2 shows two asymmetric cells considered in this paper composed of circular sections, called sub-cell a and sub-cell b, and has properties of Young's modulus $E = E_a = E_b$, density $\rho = \rho_a = \rho_b$ and cross-section area S_a and S_b, with external diameters respectively, d_a and d_b. The difference between the structures in Fig. 2(a) and Fig. 2(b), is that the first is a solid cell, and the second is a hollow cell with an internal diameter d_{int}. As the greatest reduction in the transmissibility for the lowest attenuation band, occurs when the sub-cells lengths are equal [12], it is assumed that $l_a = l_b = l$. The objective of this paper is to evaluate the performance of both types of cells in terms of vibration transmission reduction and to compare the advantages of each structure from a practical point of view.

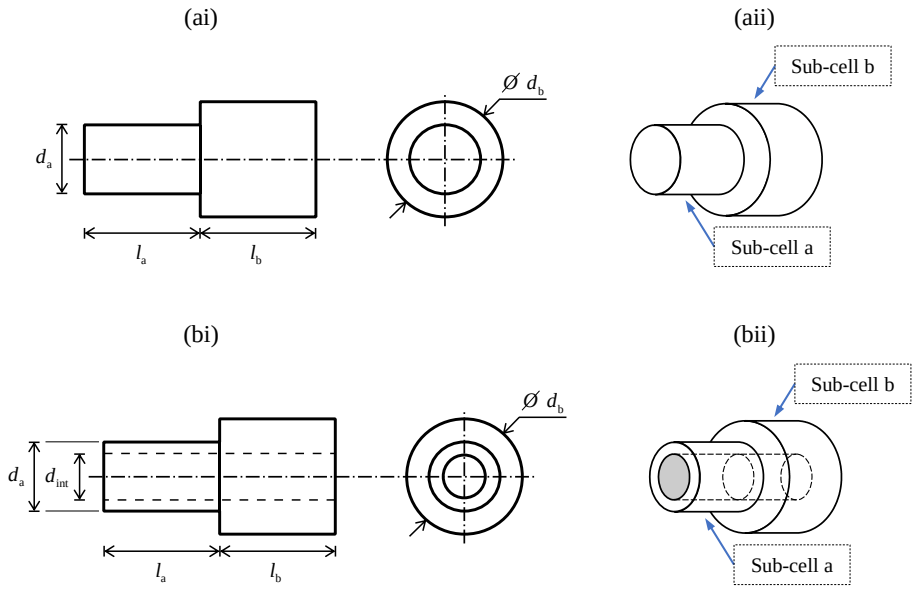

Figure 2. Drawings for a stepped rod cell. (a) solid, $d_{int} = 0$; (b) hollow, $d_{int} \neq 0$. (i) section views (ii)isometric views

Considering Fig. 1, the relationship between the forces and normalised displacements at each end of a structure with N cells is given by,

$$\begin{Bmatrix} F_R^{[N]} \\ \dfrac{U_R^{[N]}}{ES_a k} \end{Bmatrix} = \left[\mathbf{T}_{cell}\right]^N \begin{Bmatrix} F_R^{[1]} \\ \dfrac{U_L^{[1]}}{ES_a k} \end{Bmatrix}, \tag{1}$$

where $k = \frac{\omega}{c}$ is the longitudinal wavenumber, where $c = \sqrt{\frac{E}{\rho}}$ is the phase velocity; $\mathbf{T}_{cell}$ is the cell transfer matrix, given by the product of the individual transfer matrices of each sub-cell $\mathbf{T}_{\mathrm{a}} = \begin{bmatrix} \cos(kl) & -\sin(kl) \\ \sin(kl) & \cos(kl) \end{bmatrix}$ and $\mathbf{T}_{\mathrm{b}} = \begin{bmatrix} \cos(kl) & -\alpha \sin(kl) \\ \alpha^{-1} \sin(kl) & \cos(kl) \end{bmatrix}$, in which $\alpha = \frac{\text{cross-sectional area of b}}{\text{cross-sectional area of a}} = \frac{S_{\mathrm{b}}}{S_{\mathrm{a}}}$ is the area ratio for a generic cell, thus

$$\mathbf{T}_{cell} = \mathbf{T}_{\mathrm{b}}\mathbf{T}_{\mathrm{a}} = \begin{bmatrix} \cos^2(kl) - \alpha \sin^2(kl) & -\frac{(\alpha+1)}{2}\sin(2kl) \\ \frac{(\alpha+1)}{2\alpha}\sin(2kl) & \frac{\alpha\cos^2(kl) - \sin^2(kl)}{\alpha} \end{bmatrix}. \tag{2}$$

The displacement transmissibility for a structure with *N* cells is given by

$$\left.\frac{U_R^{[N]}}{U_L^{[1]}}\right|_{F_R=0} = \frac{1}{\tilde{T}_{2,2}}, \tag{3}$$

where $\tilde{T}_{2,2}$ is the element 2,2 of the inverse of the transfer matrix of the complete finite array $\left[\mathbf{T}_{cell}{}^{N}\right]^{-1}$. For a single cell [12],

$$\left|\frac{U_R^{[1]}}{U_L^{[1]}}\right| = |T| = \frac{2}{(\alpha+1)\cos(2kl) - (\alpha-1)}. \tag{4}$$

The area ratio can be written as a function of the diameters. For the solid cell in Fig. 2(a) this is given by

$$\alpha_1 = \frac{S_{\mathrm{b}}^{[\mathrm{Solid}]}}{S_{\mathrm{a}}^{[\mathrm{Solid}]}} = \frac{d_{\mathrm{b}}{}^2}{d_{\mathrm{a}}{}^2} \tag{5}$$

and for the hollow cell in Fig. 2(b) by

$$\alpha_2 = \frac{S_{\mathrm{b}}^{[\mathrm{Hollow}]}}{S_{\mathrm{a}}^{[\mathrm{Hollow}]}} = \frac{d_{\mathrm{b}}^2 - d_{\mathrm{int}}^2}{d_{\mathrm{a}}^2 - d_{\mathrm{int}}^2}. \tag{6}$$

Note that the maximum internal diameter is limited such that $d_{\mathrm{int}} < d_{\mathrm{a}}$. Thus, it is convenient to write α_2 in terms of $\beta = \frac{d_{\mathrm{int}}}{d_{\mathrm{a}}}$, which has to be less than unity, so that

$$\alpha_2 = \frac{\alpha_1 - \beta^2}{1 - \beta^2}. \tag{7}$$

Equation (7) shows the influence of the internal diameter on the area ratio, having as reference the solid structure.

3 Results and discussions

To illustrate the effect of using a hollow element on vibration transmission through a periodic structure, the displacement transmissibility for a single cell and for a structure with 3 cells is plotted in Fig. 3 as a function of l/λ, where λ is wavelength and is related to the wavenumber by $k = 2\pi/\lambda$. A loss factor of $\eta = 0.01$ is assumed.

Note that a hollow element causes a reduction in the transmissibility, with a minimum $\left(|T|_{\min}\right)$ highlighted by the black squares, and an increase in the attenuation band, highlighted by the dashed green lines. The attenuation band is defined by the region where the transmissibility is less than unity. This is called the bandwidth (BW). This region is a maximum for a single cell and reduces as the number of cells increases, finally coinciding with the stop band for an infinite structure when N is very large. The reduction in the attenuation band between one and three cells can be seen by comparing Figs. 3(a) and Fig. 3(b). The green circles give the lower and upper bounds. The improved attenuation for the hollow structure observed in Fig. 3 is due to the increase in the area ratio of the structure.

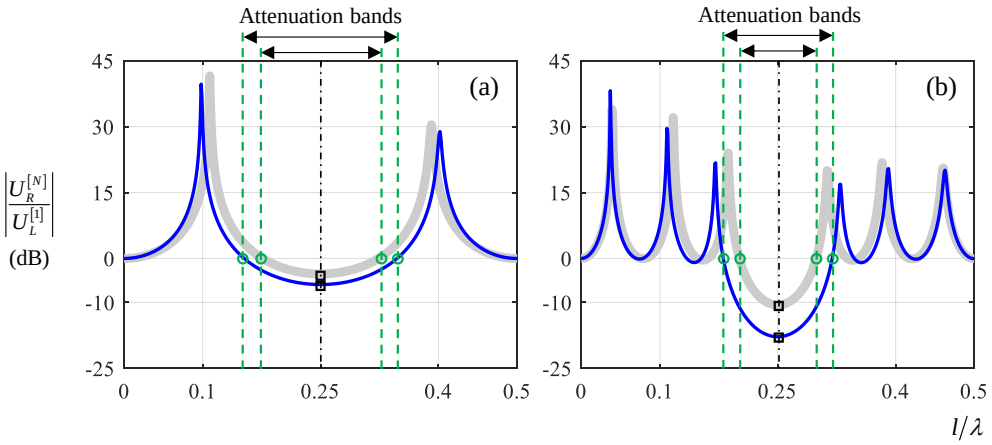

Figure 3. Displacement transmissibility for structures with $\alpha_1 = 1.5$, solid structure, thick grey line; and hollow structure with $\beta = 0.7$, thin blue line. (a) $N = 1$ and (b) $N = 3$.

The minimum transmissibility occurs at $\left.\frac{l}{\lambda}\right|_{\min} = \frac{1}{4}$, and at this frequency Eq. (5) become

$$\left|T\right|_{\min} = \frac{1}{\alpha}. \tag{8}$$

When this condition is applied in Eq. (2), the off-diagonal terms in the transfer matrix of a single cell are 0. Thus, at this frequency there is no cross coupling between the displacements and the force, and the minimum transmissibility for *N* cells is given by [12],

$$\left|\frac{U_R^{[N]}}{U_L^{[1]}}\right|_{\min} = \frac{1}{\alpha^N}, \tag{9}$$

or in terms of maximum attenuation in dB,

$$\left|A\right| = 20\log_{10}\left(\alpha\right)N. \tag{10}$$

Another significant effect of using hollow cells is mass reduction. The mass for a solid element is given by $m_1 = \rho l\left(S_{\mathrm{a}}^{[\mathrm{Solid}]} + S_{\mathrm{b}}^{[\mathrm{Solid}]}\right) = \rho l S_{\mathrm{a}}^{[\mathrm{Solid}]}\left(1+\alpha_1\right)$ and $m_2 = \rho l\left(S_{\mathrm{a}}^{[\mathrm{Hollow}]} + S_{\mathrm{b}}^{[\mathrm{Hollow}]}\right) = \rho l S_{\mathrm{a}}^{[\mathrm{Hollow}]}\left(1+\alpha_2\right)$ so the mass reduction can be expressed as,

$$1 - \frac{m_2}{m_1} = \frac{2\beta^2}{1+\alpha_1}. \tag{11}$$

The effect of reducing the mass (or increasing the internal diameter of the hollow cell) on the minimum transmissibility and bandwidth for structures with different numbers of cells is shown in Fig. 4. Again, the increase in the attenuation band is observed, as an effect of the increase in β, and the reduction in the minimum transmissibility and bandwidth, due to the increase in *N*. The black dotted line highlights the points where $\beta = 0.7$, as in the blue line in Fig. 3, note that the mass reduction is approximately 40%. The results shown in Figs. 3 and 4, consider $\alpha_1 = 1.5$ as the reference area ratio. Figs. 5 and 6 show the effect on the bandwidth, and on mass reduction and maximum vibration attenuation of a single cell as a function of α_1, for different values of β.

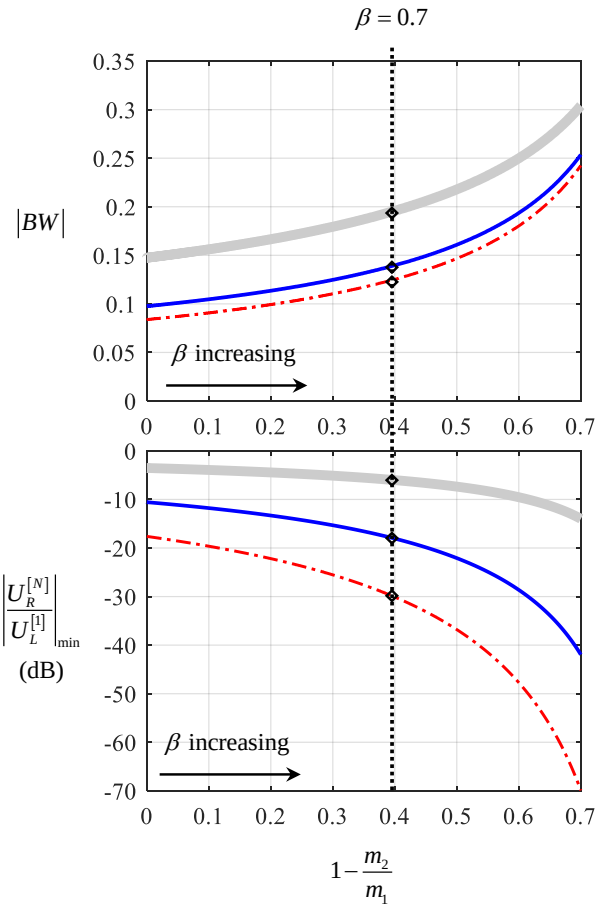

Figure 4. Effect of reducing mass by increasing the internal diameter of the hollow structure on (a) the bandwidth; and (b) minimum transmissibility, considering $N = 1$, thick grey line; $N = 3$ thin blue line, and $N = 5$ thin red dash-dot line.

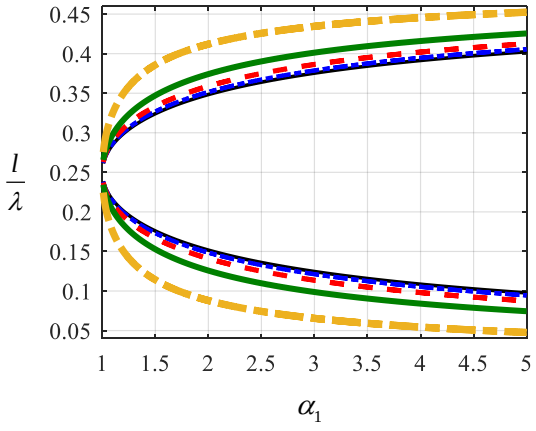

Figure 5. Lower and upper bands of the attenuation band for a single cell, as a function of solid cell area ratio, for $\beta = 0.1$, thin black line; $\beta = 0.3$, thin blue dash-dot line; $\beta = 0.5$, thin red dash line; $\beta = 0.7$, thick solid green line; and $\beta = 0.9$, thick yellow dash-dot line.

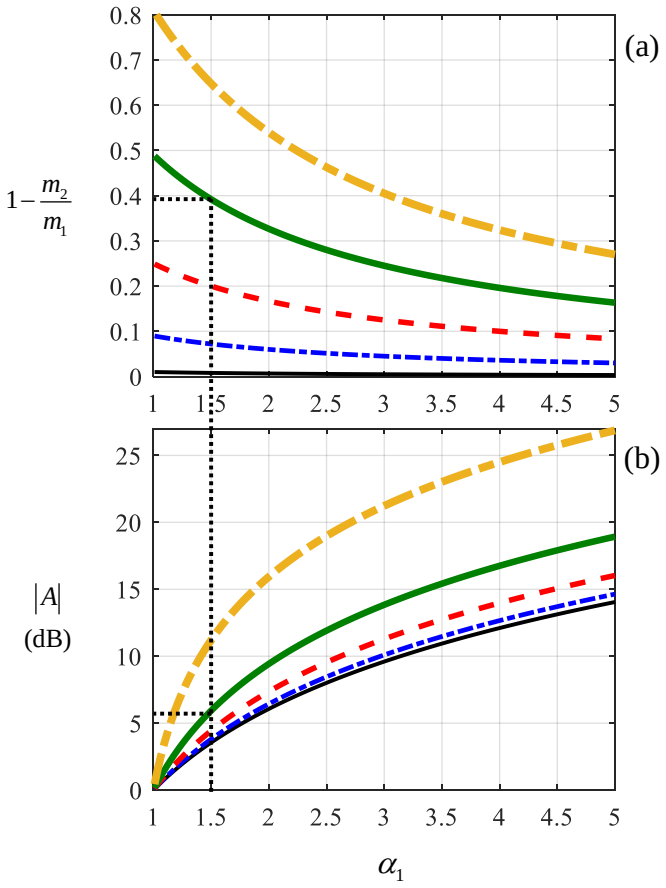

Figure 6. The effect on mass reduction and maximum vibration attenuation as function of the solid single cell area ratio for $\beta = 0.1$, thin black line; $\beta = 0.3$, thin blue dash-dot line; $\beta = 0.5$, thin red dash line; $\beta = 0.7$, thick solid green line; and $\beta = 0.9$, thick yellow dash-dot line. (a) Mass reduction; (b) maximum attenuation.

Figures 5 and 6 can be used to predict the effects in terms of attenuation and mass reduction of a hollow cell compared to a solid cell. Note that the black dotted lines mark the mass reduction and maximum attenuation respectively, for a cell whose internal diameter is $d_{\text{int}} = 0.7 d_{\text{a}}$ and $\alpha_1 = 1.5$, in a condition equivalent to the plots shown in Fig. 3. Equations (11) and (13) show that, in addition to the considerable mass reduction, the hollow cell has a maximum attenuation of approximately 5.9 dB, while the solid cell is approximately 3.5 dB, which corresponds to a reduction in minimum transmissibility of 24%. The increase in bandwidth is also evident in Fig. 4(a) and Fig. 5. Thus, instead of increasing the number of cells to achieve a certain vibration attenuation performance, another option is to change the area ratio by using hollow cells, provided that the strength requirements are not compromised.

4 Conclusions

A study on asymmetric periodic cells has been considered in this work, with solid and hollow rod configurations. From the transfer matrix method, expressions have been developed as a function of the internal diameter of the hollow rod. They have been used to study the vibration attenuation and mass reduction achievable in a structure consisting of a finite array of rods. The results showed that the application of hollow rather than solid periodic rods results in both an increase in the vibration attenuation and a reduction in mass. For the range of parameters used in the study, the minimum transmissibility was reduced by approximately 24%, and the bandwidth in which attenuation occurs increased by 33%, compared to a solid cell. There is also a significant reduction in the structural mass, of about 40%.

Acknowledgements. The authors would like to acknowledge the financial support of the São Paulo Research Foundation (FAPESP), grant numbers 2018/ 15894-0, 2019/19335-9 and 2020/00659-6.

Authorship statement. The authors hereby confirm that they are the sole liable persons responsible for the authorship of this work, and that all material that has been herein included as part of the present paper is either the property (and authorship) of the authors, or has the permission of the owners to be included here.

References

[1] M.I. Hussein, M.J. Leamy, M. Ruzzene, Dynamics of Phononic Materials and Structures: Historical Origins, Recent Progress, and Future Outlook, Appl. Mech. Rev. 66 (2014). https://doi.org/10.1115/1.4026911.

[2] D.M. Mead, Wave propagation in continuous periodic structures: research contributions from Southampton, 1964--1995, J. Sound Vib. 190 (1996) 495–524.

[3] X. Wu, L. Sun, S. Zuo, P. Liu, H. Huang, Vibration reduction of car body based on 2D dual-base locally resonant phononic crystal, Appl. Acoust. 151 (2019) 1–9. https://doi.org/10.1016/j.apacoust.2019.02.020.

[4] X. Wu, Y. Kong, S. Zuo, P. Liu, Research on multi-band structural noise reduction of vehicle body based on two-degree-of-freedom locally resonant phononic crystal, Appl. Acoust. 179 (2021) 108073. https://doi.org/10.1016/J.APACOUST.2021.108073.

[5] X. Zhang, H. Zhou, W. Shi, F. Zeng, H. Zeng, G. Chen, Vibration Tests of 3D Printed Satellite Structure Made of Lattice Sandwich Panels, Https://Doi.Org/10.2514/1.J057241. 56 (2018) 4213–4217. https://doi.org/10.2514/1.J057241.

[6] F. Wang, Y. Lu, H.P. Lee, X. Ma, Vibration and noise attenuation performance of compounded periodic struts for helicopter gearbox system, J. Sound Vib. 458 (2019) 407–425. https://doi.org/10.1016/j.jsv.2019.06.037.

[7] G. Totaro, Z. Gürdal, Optimal design of composite lattice shell structures for aerospace applications, Aerosp. Sci. Technol. 13 (2009) 157–164. https://doi.org/10.1016/J.AST.2008.09.001.

[8] A. Hvatov, S. Sorokin, Free vibrations of finite periodic structures in pass- and stopbands of the counterpart infinite waveguides, J. Sound Vib. 347 (2015). https://doi.org/10.1016/j.jsv.2015.03.003.

[9] P.G. Domadiya, E. Manconi, M. Vanali, L. V Andersen, A. Ricci, Numerical and experimental investigation of stopbands in finite and infinite periodic one-dimensional structures, J. Vib. Control. 22 (2016) 920–931. https://doi.org/10.1177/1077546314537863.

[10] A. Obradović, S. Šalinić, A. Grbović, Mass minimization of an Euler-Bernoulli beam with coupled bending and axial vibrations at prescribed fundamental frequency, Eng. Struct. 228 (2021). https://doi.org/10.1016/j.engstruct.2020.111538.

[11] P.J.P. Gonçalves, M.J. Brennan, V.G. Cleante, Predicting the stopband behaviour of finite mono-coupled periodic structures from the transmissibility of a single element, Mech. Syst. Signal Process. 154 (2021). https://doi.org/10.1016/j.ymssp.2020.107512.

[12] J.P. Carneiro Jr, M.J. Brennan, P.J.P. Gonçalves, V.G. Cleante, D.D. Bueno, R.B. Santos, On the attenuation of vibration using a finite periodic array of rods comprised of either symmetric or asymmetric cells, J. Sound Vib. 511 (2021). https://doi.org/10.1016/j.jsv.2021.116217.